ELSEVIER

Thermochimica Acta 262 (1995) 129–144

thermochimica acta

The effect of procedural variables and mechanical activation on the thermal decomposition of calcite. An approach by experimental design

G.N. Karagiannis, T.C. Vaimakis *, A.T. Sdoukos

University of Ioannina, Department of Chemistry, P.O. Box 1186, 45110 Ioannina, Greece

Received 30 September 1994; accepted 21 February 1995

Abstract

Second-order orthogonal experimental design has been used to examine the effect of mechanical activation, mass sample, heating rate and molar fraction of carbon dioxide in the environmental atmosphere on the thermal decomposition of calcite.

The mathematical model of the activation energy (E_a) for various mechanisms was examined by the Coats–Redfern equation using the best-fit procedure and the method of the shape of the TG/DTG curves. The best-fit procedure gave the second-order reaction mechanism (F2) as the predominant mechanism while the shape method gave the contacting area geometrical mechanism (R2) and the two-dimensional diffusion mechanism (D2) as the predominant mechanisms.

The mathematical models for the change of enthalpy (ΔH) and the temperature of the maximum rate of decomposition (T_{max}) were found, but unfortunately only the T_{max} model was of significance.

Keywords: Activation energy; Calcite; Decomposition; Experimental design

1. Introduction

In the last twenty years many thermoanalytical techniques have been widely used for the study of the thermal decomposition of solids and the understanding of the mechanisms which control these processes. Several techniques have been used to analyse the thermogravimetric curves, the most common being the Coats–Redfern method [1]. The overall kinetics of the thermal decomposition of solids is largely

* Corresponding author.

SSDI 0040-6031(95)02320-8

affected by procedural variables, i.e. external factors such as heating rate, particle size, sample weight, linear velocity of purge gas, and the pressure and composition of the atmosphere. Internal factors also have an effect on the decomposition process. The most important ones are the energy of the substrates and products, the lattice defects, the mobility of crystal lattice elements and the induced energy from size reduction processes (mechanical activation). The latter can also represent an external factor, i.e. the time of mechanical activation, and the charge and environment of grinding. It is also very important to find a way of interpreting research data by a mathematical model which can represent the effect on the internal and external factors. The statistical design of experiments is a relevant technique which according to Murphy [2] has four benefits: (a) it can give more information per experiment than unplanned approaches, (b) an organized approach toward the collection and analysis of information, (c) an assessment of information reliability in the light of experimental and analytical variations and (d) the capability of recognising interactions among experimental variables. The thermal decompositions of calcite and calcium carbonate have been studied by numerous authors under isothermal [3–7] and non-isothermal [3, 7–14] conditions and by constant rate thermal analysis [15]. The combination of various experimental conditions has led to a very large range of kinetic parameter values.

In this paper, we report the effect of sample size, heating rate, partial pressure of carbon dioxide, and time of mechanical activation on the thermal decomposition of calcite, using a full second-order statistical experimental design, which usually provides a good approximation of the true behaviour of a given system.

2. Experimental and results

A natural calcite, from the Epirus (Greece) area, was crushed to under 500 μm particle size using a jaw crusher; 10 g of crushed calcite with 5 ml water were transferred into a 250 ml capacity stainless-steel cylindrical bowl with 50 stainless steel balls of 10 mm diameter and ground using a Fritzch pulverisette 5 planetary mill for the necessary times (Table 1, factor z_1).

Thermal analysis of ground calcite was carried out using a Chyo-TRDA$_3$H derivatograph with simultaneous recording of temperature (T), thermogravimetry (TG), differential thermogravimetry (DTG) and differential thermal analysis (DTA). All the analyses used α-Al_2O_3 as a blank and the other variables were mass sample, heating rate and carbon dioxide molar fraction in its mixture with nitrogen (Table 1, factors z_2, z_3 and z_4 respectively). The flow rate of CO_2/N_2 mixtures for all the runs was 150 ml min^{-1} at atmospheric pressure. Tables 1 and 2 show the experimental conditions which reflect a statistical experimental design.

2.1. Experimental design

We used a second-order orthogonal factorial experimetal design [2, 16] to obtain the geometrical portrait of response surfaces for the activation energy (E_a), the change of enthalpy (ΔH) and the temperature at maximum rate decomposition (T_{max}) by means

Table 1
The principal level and incremental changes in the factors

Factor	Mechanical activation time/min	Mass/g	Heating rate/(°C min^{-1})	Molar fraction of CO_2
Natural scale/ dimensionless coordinate[a]	z_1/x_1	z_2/x_2	z_3/x_3	z_4/x_4
Basic level	90/0	100/0	5.93/0	0.5/0
Unit	30/1	50/1	2.96/1	0.2/1
Upper level	120/+1	150/+1	8.9/+1	0.7/+1
Lower level	60/−1	50/−1	2.97/−1	0.3/−1
Star arm				
Upper level[a]	132.4/ +1.414	160/ +1.414	10.11/ +1.414	0.78/ +1.414
Lower level[a]	47.6/−1.414	40/−1.414	1.74/−1.414	0.22/−1.414

[a] $x_i = (z_i - z_i^0)/\Delta z_i$.

of the estimated regression equation

$$\hat{y} = b_0 + \sum_1^n b_i x_i + \sum_1^{n'} b_{ij} x_i x_j + \sum_1^n b_{ii} x_i^2 \quad n' = n(n-1)/2 \tag{1}$$

where b_0, b_i, b_{ii}, and b_{ij} are the free term, linear term, quadratic term and interaction term coefficients, $i \neq j$. The coefficients were calculated from the equation

$$b_{ij} = \frac{\sum_1^N x_{ij} y_u}{\sum_1^N x_{ij}^2} \tag{2}$$

The significance of the coefficients was tested on the basis of the Student t-test for a level of $p = 0.05$ or 95% confidence and an error mean square (S_e^2) which was found from three repeated observations (B_1, B_2 and B_3, see Table 4, below) at the centre point of the design ($\bar{y}_i^0$) (here, for $f = 3 - 1 = 2$ degrees of freedom, $t = 4.30$)

$$S_e^2 = \frac{\sum^3 (y_i^0 - \bar{y}_i^0)^2}{2} \tag{3}$$

To test the estimated model, i.e. the equation after eliminating insignificant coefficients, we used Fisher's variance ratio (F-test)

$$F = S_r^2 / S_e^2 \tag{4}$$

Table 2
The second-order orthogonal design matrix for $k = 4$

Run	x_0	x_1	x_2	x_3	x_4	x_1'[a]	x_2'	x_3'	x_4'	x_1x_2	x_1x_3	x_1x_4	x_2x_3	x_2x_4	x_3x_4
1	+1	+1	+1	+1	+1	0.2	0.2	0.2	0.2	+1	+1	+1	+1	+1	+1
2	+1	−1	−1	+1	+1	0.2	0.2	0.2	0.2	+1	−1	−1	−1	−1	+1
3	+1	+1	−1	−1	+1	0.2	0.2	0.2	0.2	−1	−1	+1	+1	−1	−1
4	+1	−1	+1	−1	+1	0.2	0.2	0.2	0.2	−1	+1	−1	−1	+1	−1
5	+1	+1	−1	+1	−1	0.2	0.2	0.2	0.2	−1	+1	−1	−1	+1	−1
6	+1	−1	+1	+1	−1	0.2	0.2	0.2	0.2	−1	−1	+1	+1	−1	−1
7	+1	+1	+1	−1	−1	0.2	0.2	0.2	0.2	+1	−1	−1	−1	−1	+1
8	+1	−1	−1	−1	−1	0.2	0.2	0.2	0.2	+1	+1	+1	+1	+1	+1
9	+1	+1	−1	+1	+1	0.2	0.2	0.2	0.2	−1	+1	+1	−1	−1	+1
10	+1	−1	+1	+1	+1	0.2	0.2	0.2	0.2	−1	−1	−1	+1	+1	+1
11	+1	+1	+1	−1	+1	0.2	0.2	0.2	0.2	+1	−1	+1	−1	+1	−1
12	+1	−1	−1	−1	+1	0.2	0.2	0.2	0.2	+1	+1	−1	+1	−1	−1
13	+1	+1	+1	+1	−1	0.2	0.2	0.2	0.2	+1	+1	−1	+1	−1	−1
14	+1	−1	−1	+1	−1	0.2	0.2	0.2	0.2	+1	−1	+1	−1	+1	−1
15	+1	+1	−1	−1	−1	0.2	0.2	0.2	0.2	−1	−1	−1	+1	+1	+1
16	+1	−1	+1	−1	−1	0.2	0.2	0.2	0.2	−1	+1	+1	−1	−1	+1
17	+1	0	0	0	0	−0.8	−0.8	−0.8	−0.8	0	0	0	0	0	0
18	+1	+1.414	0	0	0	1.2	−0.8	−0.8	−0.8	0	0	0	0	0	0
19	+1	−1.414	0	0	0	1.2	−0.8	−0.8	−0.8	0	0	0	0	0	0
20	+1	0	+1.414	0	0	−0.8	1.2	−0.8	−0.8	0	0	0	0	0	0
21	+1	0	−1.414	0	0	−0.8	1.2	−0.8	−0.8	0	0	0	0	0	0
22	+1	0	0	+1.414	0	−0.8	−0.8	1.2	−0.8	0	0	0	0	0	0
23	+1	0	0	−1.414	0	−0.8	−0.8	1.2	−0.8	0	0	0	0	0	0
24	+1	0	0	0	+1.414	−0.8	−0.8	−0.8	1.2	0	0	0	0	0	0
25	+1	0	0	0	−1.414	−0.8	−0.8	−0.8	1.2	0	0	0	0	0	0

[a] $x_i' = x_i^2 - (\sum x_{iu}^2)/N$.

where S_r^2 is the residual mean square

$$S_r^2 = \frac{\sum_{1}^{N} (y_u - \hat{y}_u)^2}{N - l} \tag{5}$$

where l is the number of significant coefficients.

Table 1 shows the centre point of design or basic level (z_1^0, z_2^0, z_3^0 and z_4^0, $z_i^0 = (z_{i\max} + z_{i\min})/2$), the change interval or unit on the axis (Δz_1, Δz_2, Δz_3 and Δz_4, $\Delta z_i^0 = (z_{i\max} + z_{i\min})/2$), the upper and lower levels ($z_{i\max}$ and $z_{i\min}$) and also the definition of the factors. Table 2 shows the matrix of a second-order orthogonal design for $k = 4$. The number of experiments was 25 and the star arm was 1.414.

2.2. Kinetic analysis

The kinetic analyses of the thermal decomposition of calcite was studied using the modified Coats–Redfern method, based on Eq. (1), for various mechanisms [17] as listed in Table 3

$$\ln(g(\alpha)/T^2) = \ln\left[\left(\frac{ZR}{\beta E_a}\right)\left(1 - \frac{2RT}{E_a}\right)\right] - \frac{E_a}{RT} \tag{6}$$

where $g(\alpha)$ (some authors use the symbol $f(\alpha)$) is the integral of the inverse function which describes the dependence of $d\alpha/dt$ on α, α is the reacted molar fraction, t the time,

Table 3
Classification of solid-state rate expressions

Symbol		$g(\alpha)$
Acceleratory α–time curves		
Pn	Power law ($n = 1, 2, 3, 4$)	$\alpha^{1/n}$
Sigmoid α–time curves		
An	Avrami–Erofe'ev (Random nucleation $n = 2, 3, 4$)	$[-\ln(1-\alpha)]^{1/n}$
Deceleration α–time curves based on geometrical models		
R2	Contracting area	$1-(1-\alpha)^{1/2}$
R3	Contracting volume	$1-(1-\alpha)^{1/3}$
Deceleration α–time curves based on diffusion mechanisms		
D1	One-dimensional	α^2
D2	Two-dimensional	$(1-\alpha)\ln(1-\alpha)+\alpha$
D3	Three-dimensional, spherical symmetry; Jander equation	$[1-(1-\alpha)^{1/3}]^2$
D4	Three-dimensional, spherical symmetry; Ginstling–Brounshtein equation	$(1-2\alpha/3)-(1-\alpha)^{2/3}$
Deceleration α–time curves based on order of reaction		
F1	First order	$-\ln(1-\alpha)$
F2	Second order	$1/(1-\alpha)$

T the temperature, Z the pre-exponential factor, R the gas constant, E_a the activation energy, and β the heating rate. When $\ln(g(\alpha)/T^2)$ is plotted against $1/T$, straight lines can be drawn by the method of least squares, from which E_a, Z and the correlation coefficient are calculated. For each mechanism, the mean value of the correlation coefficients of all runs is accepted as the mean correlation coefficient (r_m). The random nucleation mechanism (A2, A3, A4) which yields the highest correlation coefficients is accepted as the predominant nucleation mechanism. Another way to choose the predominant mechanism for each run, according to Dollimore and coworkers [13, 17–19], is the shape of the TG/DTG curves. From (Fig. 1) the decomposed fraction at maximum rate decomposition (α_{max}), the DTG peak width at half height or half width (HiT-LoT), and the initial or onset temperature (T_i) and final temperature (T_f) of TG curve, we found the predominant mechanism according to Fig. 2.

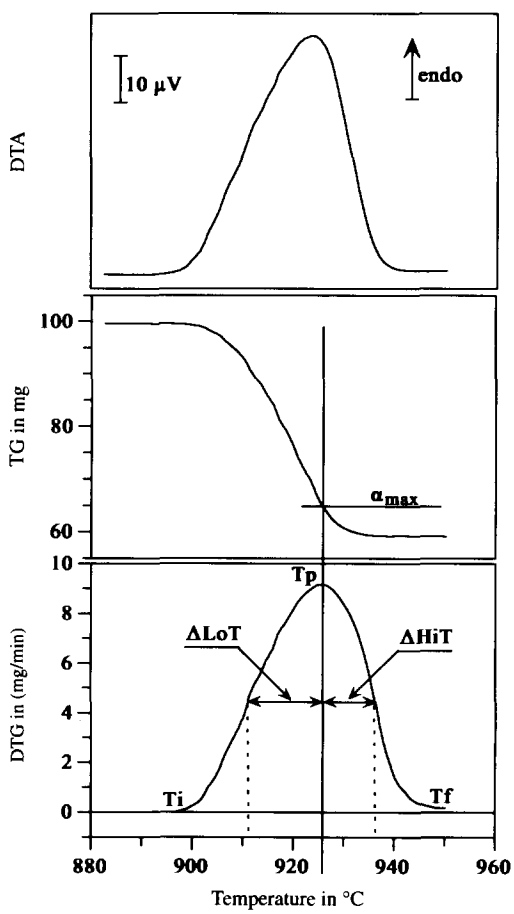

Fig. 1. TG, DTG and DTA curves of calcite using basic level conditions (see Table 1), and the schematic representation of the determination of α_{max} and the half width of the DTG peak.

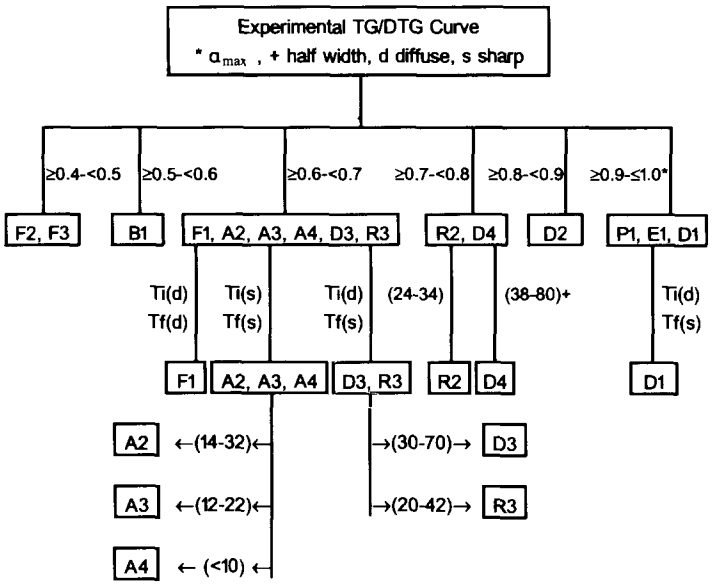

Fig. 2. Flow chart showing procedures in recognising the kinetic equations [17].

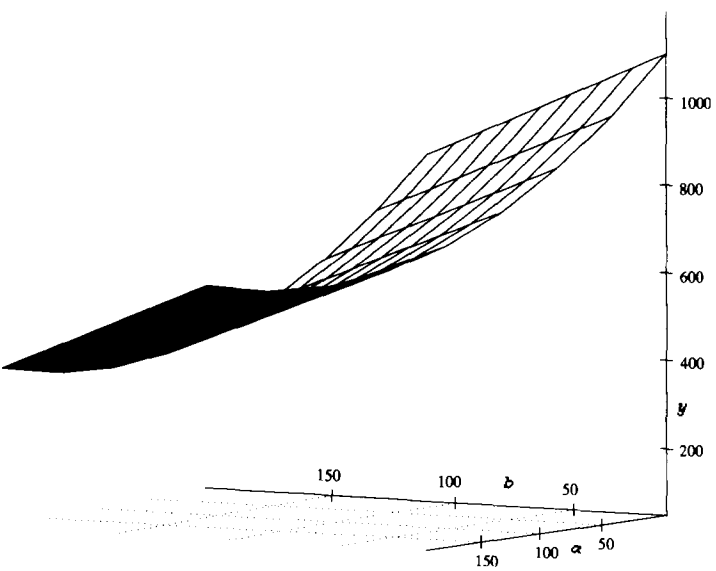

Fig. 3. The response surface of the F2 model for activation energy (y axis). The effect of activation time (z_1, a axis) and mass sample (z_2, b axis) at a heating rate of 5.93°C min^{-1} and CO_2 molar fraction 0.5.

The change of enthalpy for the calcite decomposition was determined from the peak area of the DTA curves by the equation

$$\Delta H = \frac{KsA}{\beta m} \tag{7}$$

where K is the derivatograph constant, s is the used sensitivity for the DTA measurements, A the peak area and m the mass of the sample.

3. Discussion

The highest mean correlation coefficients of the activation energy models for different mechanism (Table 4) are those of the second-order reaction model (F2) ($r_m = 0.9950$). From Table 5, the F-test indicates that only the F2 mechanism model is significant at 95% confidence. The shape method gave a relatively low value of the

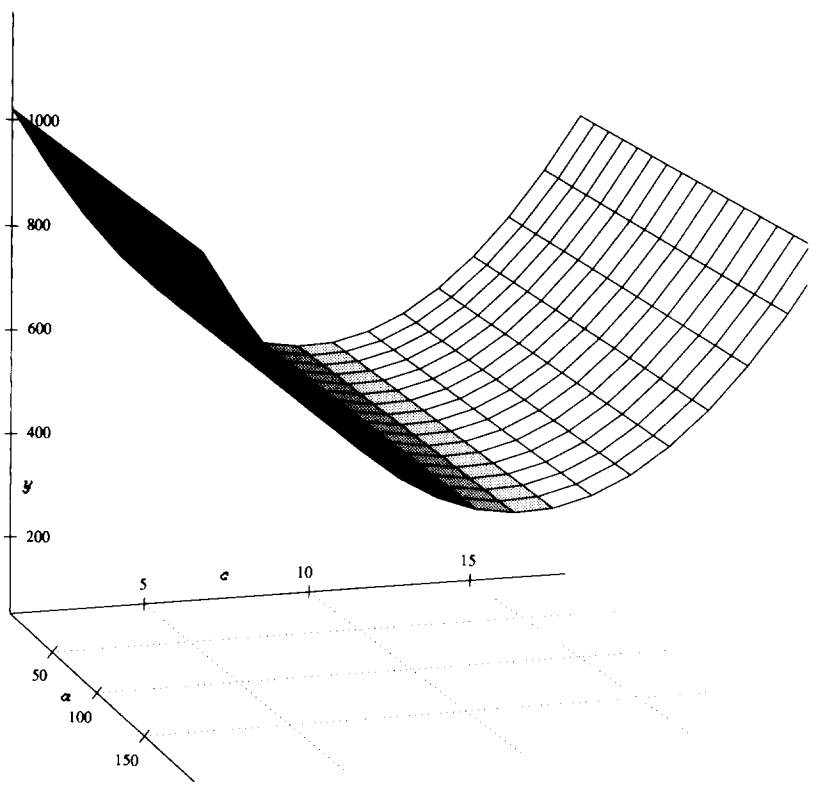

Fig. 4. The response surface of the F2 model for activation energy (y axis). The effect of activation time (z_1, a axis) and heating rate (z_3, c axis) with a sample mass of 100 mg and CO_2 molar fraction 0.5.

Table 4
The activation energies E_a, the change of enthalpies ΔH, and the temperature at the maximum rate of decomposition T_{max} for different experimental conditions

No.	E_a/kcal mol^{-1}										ΔH/ (kcal mol^{-1})	T_{max}/K
	P1	A2	R2	R3	D1	D2	D3	D4	F1	F2		
1	100	138	988	1040	724	445[a]	495	461	276	460	48.7	1216
2	165	220	1609	1688	1277	727[a]	804	752	444	785	50.1	1204
3	229	316	2258	2384[a]	576	1017	1138	1056	637	1110	147.5	1202
4	141	191	1386	1459	1015	634[a]	704	657	387	686	138.7	1206
5	172	258	1784[a]	1908	728	825	946	865	522	591	54.3	1177
6	113	160	1140[a]	1207	1324	518	583	539	325	377	48.2	1192
7	178	246	1764[a]	1861	593	791	882	821	496	540	149.1	1174
8	316	563	3060	3212[a]	928	1196	1349	1246	840	890	171.8	1163
9	164	217	1595	1671	467	630[a]	722	660	439	765	50.3	1205
10	89	120	883	928	727	426[a]	467	439	246	446	47.2	1214
11	145	199	1434	1512	369	650[a]	722	674	403	646	132.1	1203
12	250	335	2435[a]	2557	674	1112	1230	1150	675	1153	156.5	1200
13	116	159	1157	1219	480	518[a]	577	537	243	333	53.2	1193
14	239	256	1802[a]	1915	703	804	919	842	517	580	56.2	1163
15	327	436	3169	3324[a]	413	1361	1509	1410	876	925	161.6	1167
16	177	236	1725[a]	1808	669	786	866	812	476	557	159.5	1175
17/B1	162	220	1589	1672	661	732[a]	804	750	444	611	78.7	1197
18	154	210	1523[a]	1607	622	692	773	718	425	598	74.7	1198
19	157	220	1566[a]	1656	642	709	796	738	444	627	81.4	1199
20	119	161	1173[a]	1235	489	535	595	555	328	449	81.1	1202
21	242	337	3293[a]	2532	979	1081	1215	1125	679	963	88.1	1186
22	124	169	1225	1291	509[a]	558	622	579	343	475	45.9	1201
23	269	355	2595[a]	2719	1088	1184	1304	1223	715	958	282.7	1187
24	154	217	1546[a]	1636	632	670	787	728	439	618	72.6	1216
25	117	159	1158[a]	1218	483	529	587	548	323	441	88.5	1171
r_m[b]	0.9577	0.9879	0.9755	0.9803	0.9593	0.9696	0.9807	0.9738	0.9882	0.9950	–	–
B2	158	216	1590	1670	654	709	790	735	440	599	81.1	1196
B3	162	218	1594	1679	664	726	804	751	442	598	81.5	1196

[a] The predominant mechanism accordingly the shape of the TG/DTG curve.
[b] Mean correlation coefficient.

Table 5
The estimated model on dimensionless coordinates and natural scale variables, and the statistical test of the model for the activation energy E_a, the change of enthalpy ΔH, and the temperature at the maximum rate of decomposition T_{max}

		Model	$F_{exp.}$	f_R	F_{table}
E_a	P1	$\hat{y} = 177 - 3.2x_1 - 48.9x_2 - 40.5x_3 - 15.3x_4 + 13.5x_2' + 21.4x_3' - 8.8x_4' + 6.1x_1x_2 - 3.1x_1x_3 + 9.9x_2x_3 + 8.4x_2x_4 + 6.9x_3x_4$ $\hat{y} = 602 - 0.3z_1 - 12.9z_2 - 52.1z_3 - 11.4z_4 + 0.005z_2^2 + 2.4z_3^2 - 219z_4^2 + 0.004z_1z_2 - 0.034z_1z_3 + 0.067z_2z_3 + 0.84z_2z_4 + 11.7z_3z_4$	74.91	12	19.41
	A2	$\hat{y} = 244 - 6.4x_1 - 70.2x_2 - 62.9x_3 - 24.9x_4 + 3.8x_1' + 21.0x_2' + 27.5x_3' - 9.6x_4' + 11.2x_1x_2 + 9.0x_1x_3 + 7.3x_1x_4 + 25.2x_2x_3 + 16.9x_2x_4 + 18.6x_3x_4$ $y = 1176 - 2.9z_1 - 5.6z_2 - 100z_3 - 339z_4 + 0.004z_1^2 + 0.008z_2^2 + 3.1z_3^2 - 240z_4^2 + 0.007z_1z_2 + 0.1z_1z_3 + 0.7z_1z_4 + 0.2z_2z_3 + 1.7z_2z_4 + 31.4z_3z_4$	478.0	10	19.39
	R2	$\hat{y} = 410 - 107x_2 - 98.0x_3 - 29.4x_4 + 28.5x_2' + 43.7x_3' - 23.0x_4' + 4.6x_1x_2 + 1.1x_1x_3 - 2.8x_1x_4 + 29.7x_2x_3 + 12.3x_2x_4 + 20.8x_3x_4$ $\hat{y} = 1321 - 0.2z_1 - 6.5z_2 - 131z_3 + 136z_4 + 0.01z_2^2 + 5.0z_3^2 - 574z_4^2 + 0.003z_1z_2 + 0.01z_1z_3 - 0.5z_1z_4 + 0.2z_2z_3 + 1.2z_2z_4 + 35.2z_3z_4$	9238	12	19.41
	R3	$\hat{y} = 432 - 113x_2 - 102x_3 - 31.3x_4 + 30.4x_2' + 45.0x_3' - 24.1x_4' + 4.7x_1x_2 - 2.9x_1x_4 + 30.6x_2x_3 + 13.5x_2x_4 + 20.5x_3x_4$ $\hat{y} = 1393 - 0.07z_1 - 6.9z_2 - 133z_3 + 256z_4 + 0.01z_2^2 + 51.1z_3^2 - 602z_4^2 + 0.003z_1z_2 - 0.5z_1z_4 + 0.2z_2z_3 + 1.4z_2z_4 + 34.6z_3z_4$	1703	13	19.415
	D1	$\hat{y} = 711 - 150x_1 - 23.0x_2 + 18.7x_3 + 10.1x_4 + 48.0x_2' + 80.5x_3' - 40.0x_4' - 18.6x_1x_3 - 28.4x_2x_4$ $\hat{y} = 1093 - 3.7z_1 - 3.0z_2 - 83.6z_3 + 1335z_4 + 0.02z_2^2 + 9.2z_3^2 - 1001z_4^2 - 0.2z_1z_3 - 2.8z_2z_4$	621	15	19.425
	D2	$\hat{y} = 766 - 184x_2 - 177x_3 - 45.9x_4 + 43.0x_2' + 74.5x_3' - 53.9x_4' - 21.8x_1x_4 + 46.4x_2x_3 + 15.1x_2x_4 + 17.8x_3x_4$	40.9	14	19.42

		$\hat{y} = 1882 + 1.8z_1 - 9.7z_2 - 207x_3 + 1116z_4 + 0.02z_2^2 + 8.5z_3^2 - 1347z_4^2 - 3.6z_1z_4 + 0.3z_2z_3 + 1.5z_2z_4 + 30.0z_3z_4$			
	D3	$\hat{y} = 856 - 210x_2 - 193x_3 - 53.3x_4 + 52.0x'_2 + 81.0x'_3 - 57.1x'_4 - 20.3x_1x_4 + 49.0x_2x_3 + 19.3x_2x_4 + 17.2x_3x_4$	112	14	19.42
		$\hat{y} = 2144 + 1.7z_1 - 11.3z_2 - 222z_3 + 1102z_4 + 0.02z_2^2 + 9.2z_3^2 - 1429z_4^2 - 3.4z_1z_4 + 0.3z_2z_3 + 1.9z_2z_4 + 29.0z_3z_4$			
	D4	$\hat{y} = 795 - 192x_2 - 182x_3 - 48.3x_4 + 46.6x'_2 + 77.3x'_3 - 54.3x'_4 - 21.4x_1x_4 + 47.3x_2x_3 + 16.5x_2x_4 + 17.6x_3x_4$	84.9	14	19.42
		$\hat{y} = 1975 + 1.8z_1 - 10.3z_2 - 213z_3 + 1096z_4 + 0.02z_2^2 + 8.8z_3^2 - 1356z_4^2 - 3.6z_1z_4 + 0.3z_2z_3 + 1.6z_2z_4 + 29.7z_3z_4$			
E_a	F1	$\hat{y} = 478 - 2.3x_1 - 130x_2 - 115x_3 - 31.2x_4 + 32.8x'_2 + 45.7x'_3 - 28.5x'_4 - 5.4x_1x_3 + 27.1x_2x_3 + 20.8x_2x_4 + 24.0x_3x_4$	683	13	19.415
		$\hat{y} = 1512 - 0.6z_1 - 7.3z_2 - 134z_3 - 1005z_4 + 0.01z_2^2 + 5.2z_3^2 - 714z_4^2 - 0.06z_1z_3 + 0.2z_2z_3 + 2.1z_2z_4 + 40.6z_3z_4$			
	F2	$\hat{y} = 633 - 7.3x_1 - 174x_2 - 143x_3 + 75.5x_4 + 50.2x'_2 + 55.2x'_3 - 38.0x'_4 + 34.0x_2x_3 - 24.8x_2x_4$	13.2	14	19.42
		$\hat{y} = 1272 - 0.2z_1 - 7.6z_2 - 146z_3 + 1576z_4 + 0.02z_2^2 + 6.3z_3^2 - 950z_4^2 + 0.2z_2z_3 - 2.5z_2z_4$			
	Shape method	$\hat{y} = 479 - 38.9x_1 - 61.7x_3 + 45.2x_4 + 32.8x'_2 + 37.8x'_3 - 18.7x'_4 + 24.4x_1x_2 + 34.6x_1x_3 + 22.9x_1x_4 - 39.3x_2x_3 - 43.8x_2x_4 + 44.8x_3x_4$	40.9	14	19.42
		$\hat{y} = 1092 - 7.1z_1 - 0.3z_2 - 118z_3 + 340z_4 + 0.01z_2^2 + 4.3z_3^2 - 648z_4^2 + 0.02z_1z_2 + 0.4z_1z_3 + 3.8z_1z_4 - 0.3z_2z_3 - 4.4z_2z_4 + 75.6z_3z_4$			
	ΔH	$\hat{y} = 101 - 2.0x_1 - 4.1x_2 - 57.1x_3 - 5.2x_4 - 9.7x'_1 - 6.4x'_2 + 33.4x'_3 - 8.4x'_4 + 2.6x_1x_3 + 2.8x_2x_3 + 3.2x_3x_4$	34	13	19.415
		$\hat{y} = 246 + 1.7z_1 + 0.3z_2 - 71.6z_3 + 152z_4 - 0.01z_1^2 - 0.003z_2^2 + 3.8z_3^2 - 210z_4^2 - 0.03z_1z_3 + 0.02z_2z_3 + 5.5z_3z_4$			
	T_{max}	$\hat{y} = 1192 + 0.9x_1 + 5.7x_2 + 4.7x_3 + 15.5x_4 - 2.4x'_2 - 2.4x'_3 - 2.6x'_4 - 1.4x_1x_2 + 1.0x_1x_3 - 1.0x_1x_4 + 2.5x_2x_3 - 2.2x_2x_4 - 1.1x_3x_4$	10.04	14	19.42
		$\hat{y} = 1084 + 0.1z_1 + 0.4z_2 + 3.0z_3 + 191z_4 - 0.001z_2^2 - 0.3z_3^2 - 65.0z_4^2 - 0.001z_1z_2 + 0.01z_1z_3 - 0.2z_1z_4 + 0.02z_2z_3 - 0.2z_2z_4 - 1.9z_3z_4$			

correlation coefficient ($r_m = 0.9737$) and an unexpected insignificance by the F-test. Our individual experiments on calcite decomposition without mechanical activation showed a good agreement between these two methods [20]. So the predominant mechanism for calcite decomposition under these conditions is the second-order reaction. The shape of the TG/DTG curves gave the predominant mechanism as R2 for 13 runs and D2 for 8 runs. Dollimore et al. [13] found that at a heating rate of 10°C min^{-1}, the predominant mechanisms of limestone decomposition, as predicted by the shape method, were R3 and D3. Under isothermal conditions, Maciejewski and Reller [7] found that in carbon dioxide atmosphere the mechanisms were F1 and A2, while in nitrogen atmosphere it was P1. A change in the decomposition mechanism following mechanical activation has also been observed for magnesite [21] and calcite [22].

The F2 mechanism model (Table 5) predicts that all the linear terms are significant. The significant quadratic terms are those of the mass of sample (b_2), the rate of heating (b_3) and the molar fraction of CO_2 (b_4), while the significant interaction terms are b_2b_3 and b_2b_4. The influence of the activation time (z_1) on the activation energy is linear, as only the linear term is significant. The same linear influence is also apparent in Figs. 3–5 where the parallels at the activation time axis of the third response-surface illustration of model F2 are straight lines. Generally the activation energy is increased with decreasing activation time. The influence of three other factors on the activation energy is illustrated with a parabolic shape. Figs. 3, 6 and 7 show that the influence of sample

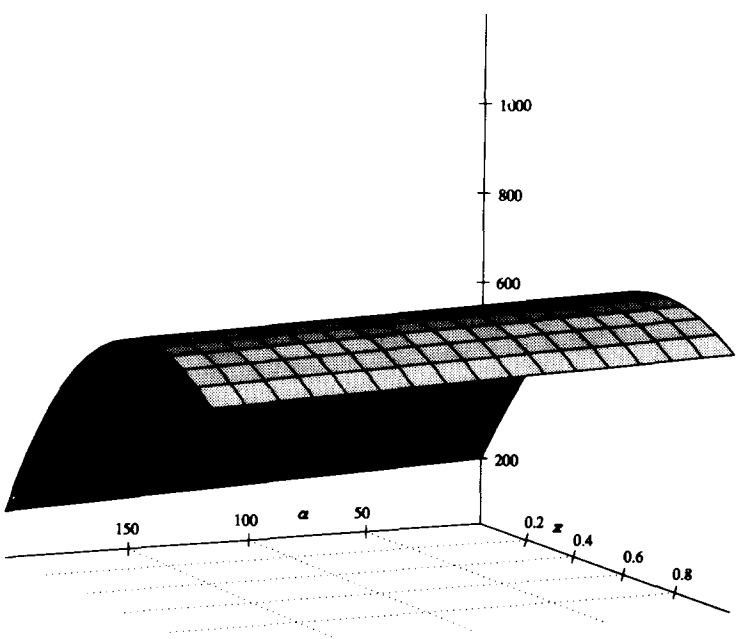

Fig. 5. The response surface of the F2 model for activation energy (y axis). The effect of activation time (z_1, a axis) and CO_2 molar fraction (z_4, z axis) with a sample mass of 100 mg and a heating rate of 5.93°C min^{-1}.

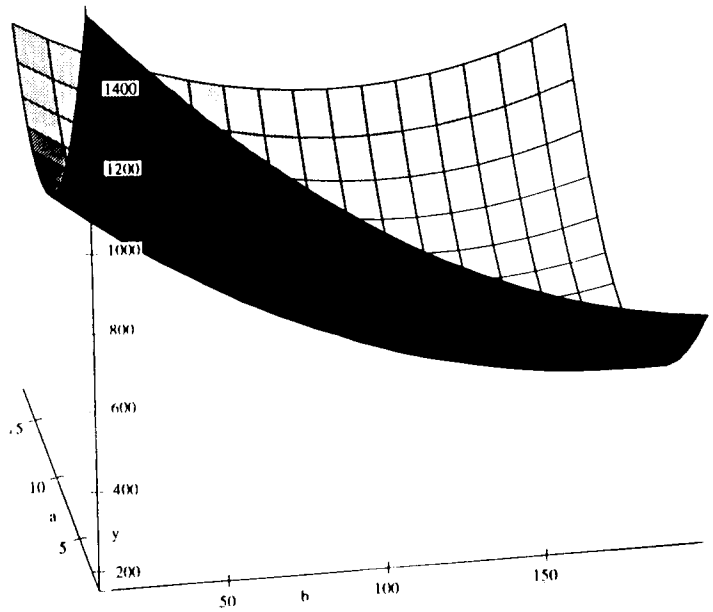

Fig. 6. The response surface of the F2 model for activation energy (y axis). The effect of sample mass (z_2, b axis) and heating rate (z_3, c axis) at an activation time of 90 min and CO_2 molar fraction 0.5.

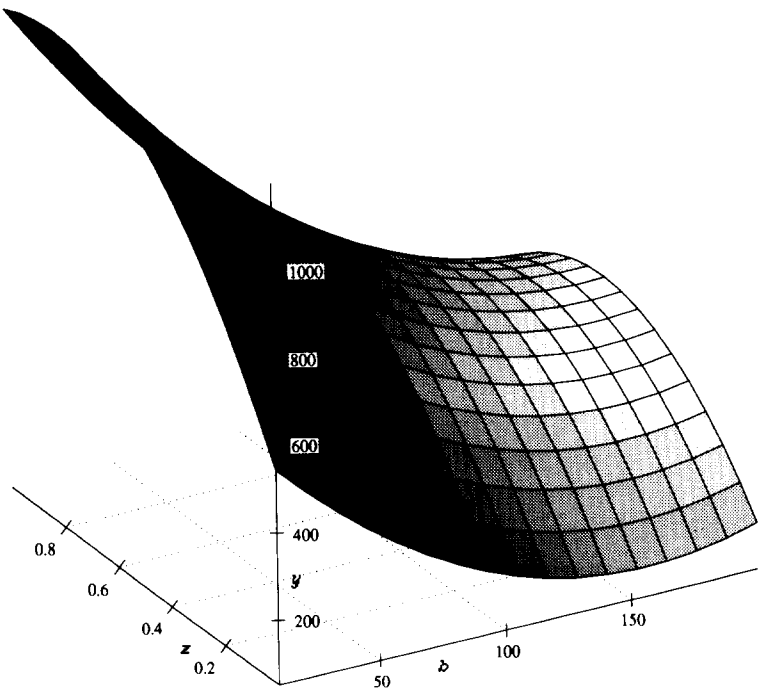

Fig. 7. The response surface of the F2 model for activation energy (y axis). The effect of sample mass (z_2, b axis) and CO_2 molar fraction (z_4, z axis) at an activation time of 90 min and a heating rate of 5.93°C min^{-1}.

mass on activation energy indicates a minimum of about 170 mg. Gallagher and Johnson [3] found that between about 1 and 17 mg, the activation energy of calcite decomposition decreased with increasing mass sample. The same effect is observed on the decomposition activation energy of $CaC_2O_4 \cdot H_2O$ [23], $[Cu(en)_2(H_2O)_2]C_2O_4$ [24] and NH_4NO_3 [25]. The influence of the heating rate on the activation energy is the same as sample mass (Figs. 4, 6 and 8), with a minimum of about $10°C\,min^{-1}$. Ninan and coworkers [23, 24] found that if the heating rate is increased, the decomposition activation energy is decreased. The inverse behaviour is shown in Figs. 5, 7 and 8 for the carbon dioxide molar fraction, with a maximum value of about 0.75. The negative signs of the $b_2 b_4$ coefficient term indicate an antagonistic influence between the z_2 and z_4 factors. Figs. 7 and 8 illustrate this antagonistic interaction by saddle response-surfaces. Surprisingly high values of E_a and T_{max} were obtained in all the runs, explained by the effect of the CO_2. High values up to 900 kcal mol^{-1} have been found by others [9, 10]. In Fig. 6, for pure nitrogen atmosphere (molar fraction of CO_2, zero) and without mechanical activation (activation time, zero), the activation energy is about 200 kcal mol^{-1} which is approx. four times more than the literature values. This could be explained by the chosen predominant mechanism. Under those conditions, the probable predominant mechanism, according to Ref. [7], was the P1 mechanism, for which (see Table 4) the values of E_a are about a quarter of those of the F2 mechanism.

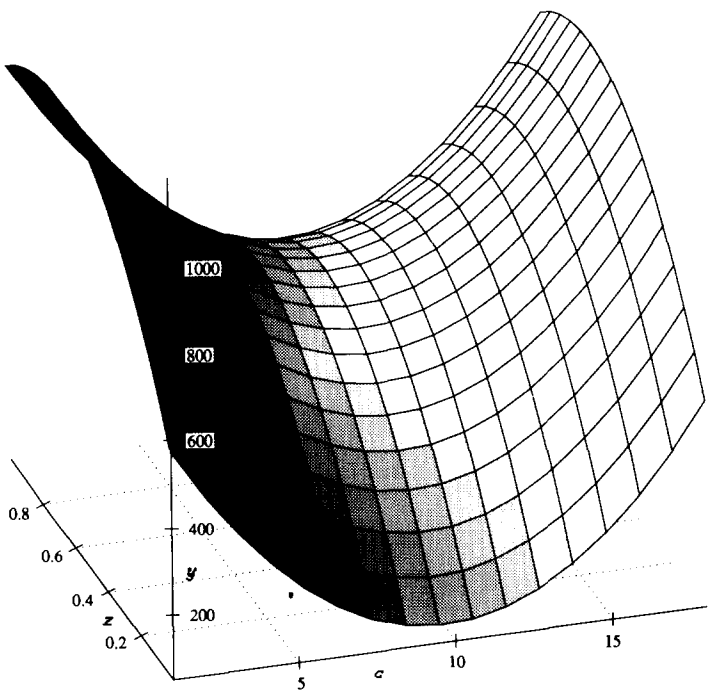

Fig. 8. The response surface of the F2 model for activation energy (y axis). The effect of heating rate (z_3, c axis) and CO_2 molar fraction (z_4, z axis) at an activation time of 90 min and a sample mass of 100 mg.

The ΔH model, as predicted by the F-test (Table 5), was not significant at the 95% confidence level.

The T_{max} model was significant at the 95% confidence level and indicated that the significant terms were those of the F2 mechanism model plus the $b_1 b_2$, $b_1 b_3$, $b_1 b_4$ and $b_3 b_4$ interaction terms. The CO_2 molar fraction (z_4) action was antagonistic to the other parameters, and the activation time (z_1) with the mass sample (z_2). The effects of the individual z_2, z_3 and z_4 parameters were not antagonistic, i.e. by increasing each one of these, the peak temperature of the DTG curves of the calcite decomposition increased [3, 12]. This change in behaviour could be attributed to the influence of the mechanical activation.

4. Conclusion

The effect of the procedural variables, i.e. mass sample, heating rate and molar fraction of carbon dioxide, on the activation energy and the temperature of the maximum rate of decomposition, as indicated by the second-order factorial experiment, was illustrated by a parabolic shape, while the effect of the mechanical activation time was linear. In particular, for the activation energy, the mass sample and the heating rate showed parabola with response surfaces opening upwards, while the CO_2 molar fraction parabola showed downward response surfaces. Accordingly, the results of the best-fit method for various mechanisms for the Coats–Redfern equation and statistical control by the F-test suggested that the predominant mechanism is the second-order reaction (F2). Therefore, the experimental design was a useful means under complex conditions to choose and explain the predominant mechanism of the decomposition of solids.

Acknowledgements

The authors acknowledge partial financial support of this study by the General Secretariat of Research and Technology of the Greek Ministry of Industry, Energy and Technology (Grant Number 91 EΔ 454). Also we wish to thank Dr. E. Papamichael for help with the 3D computer graphics.

References

[1] A.W. Coats and J.P. Redfern, Nature, 201 (1964) 68.
[2] T.D. Murphy, Chem. Engin., (1977) 168–182.
[3] P.K. Gallagher and D.W. Johnson, Thermochim. Acta, 6 (1973) 67–83.
[4] A.M. Molokozi and E. Lugwisha, Thermochim. Acta, 194 (1992) 375–383.
[5] J.-T. Lee, T.C. Keener, M. Knoderer and S.-J. Khang, Thermochim. Acta, 213 (1993) 223–240.
[6] Q. Zhong and I. Bjerle, Thermochim. Acta, 223 (1993) 109–120.
[7] M. Maciejewski and A. Reller, Thermochim. Acta, 110 (1987) 145–152.
[8] H.F. Kissinger, Anal. Chem., 29 (1957) 1702.
[9] J. Zsako and H.E. Arz, J. Therm. Anal., 6 (1974) 651–656.

[10] D. Price, N. Fatemi, D. Dollimore and R. Whitehead, Thermochim. Acta, 94 (1985) 313–322.
[11] A. Romero Salvador, E. Carcia Calvo and C. Beneitez Aparicio, Thermochim. Acta, 143 (1989) 339–345.
[12] F.W. Wilburn, J.H. Sharp, D.M. Tinsley and R.M. McIntosh, J. Therm. Anal., 37 (1991) 2003–2019.
[13] D. Dollimore, T.A. Evans, Y.F. Lee, G.P. Pee and F.W. Wilburn,Thermochim. Acta, 196 (1992) 255–265.
[14] A. Ersoy-Mericboyu, S. Kucukbayrak and R. Yavuz, Thermochim. Acta, 233 (1993) 121–128.
[15] J.M. Criado and A. Ortega, Thermochim. Acta, 195 (1992) 163–167.
[16] V. Kafarov, Cybernetic Methods in Chemistry and Chemical Engineering, Chapter II-5, Development of Mathematical Models by Experiment and Statistics, Statistical Optimization, English Translation, Mir Publishers, Moscow, 1976, pp. 167–225.
[17] D. Dollimore, Thermogravimetry, in E.L. Charsley and S.B. Warrington (Eds.), Thermal Analysis—Technique and Applications, Royal Society of Chemistry, Cambridge, 1992.
[18] D. Dollimore, T.A. Evans, Y.F. Lee and F.W. Wilburn, Thermochim. Acta, 198 (1992) 249–257.
[19] D. Dollimore, Thermochim. Acta, 203 (1992) 7–23.
[20] G. Karagiannis, T. Vaimakis and A. Sdoukos, Application of Thermal Analysis on the Study of the Thermal Decomposition Mechanism of Solids, 4th Congress of Greece–Cyprus, Chemistry and Education, Ioannina (Greece), Sept. 8–11, 1994, pp. 175–180 (in Greek).
[21] V. Jesenák, L'. Klimek, L'. Turčániová and K. Tkáčová, Effect of the Mechanical Activation on Dissociation of Magnesite, 1st International Conference on Mechanochemistry, Book of Abstracts, Kosice-Slovakia, March 23–26, 1993, p. B20.
[22] Unpublished results.
[23] K.N. Ninan, J. Therm. Anal., 35 (1989) 1267–1278.
[24] S. Mathew, C.G.R. Nair and K.N. Ninan, Thermochim. Acta, 184 (1991) 269–294.
[25] N. Koga and H. Tanaka, Thermochim. Acta, 209 (1992) 127–134.